



VU Research Portal

Paleo-elevation and EET evolution at mountain ranges: inferences from flexural modeling in the Eastern Pyrenees and Ebro Basin

Millan, H.; den Bezemer, T.; Verges, J.; Zoetemeijer, R.; Cloetingh, S.A.P.L.; Marzo, M.; Munoz, J.A.; Roca, E.; Cires, J.

published in

Marine and Petroleum Geology
1995

document version

Publisher's PDF, also known as Version of record

[Link to publication in VU Research Portal](#)

citation for published version (APA)

Millan, H., den Bezemer, T., Verges, J., Zoetemeijer, R., Cloetingh, S. A. P. L., Marzo, M., Munoz, J. A., Roca, E., & Cires, J. (1995). Paleo-elevation and EET evolution at mountain ranges: inferences from flexural modeling in the Eastern Pyrenees and Ebro Basin. *Marine and Petroleum Geology*, *12*, 917-928.

General rights

Copyright and moral rights for the publications made accessible in the public portal are retained by the authors and/or other copyright owners and it is a condition of accessing publications that users recognise and abide by the legal requirements associated with these rights.

- Users may download and print one copy of any publication from the public portal for the purpose of private study or research.
- You may not further distribute the material or use it for any profit-making activity or commercial gain
- You may freely distribute the URL identifying the publication in the public portal ?

Take down policy

If you believe that this document breaches copyright please contact us providing details, and we will remove access to the work immediately and investigate your claim.

E-mail address:

vuresearchportal.ub@vu.nl

Palaeo-elevation and effective elastic thickness evolution at mountain ranges: inferences from flexural modelling in the Eastern Pyrenees and Ebro Basin

H. Millán*

Department of Geology, University of Zaragoza, Zaragoza, Spain

T. Den Bezemer

Faculty of Earth Sciences, Vrije University, Amsterdam, the Netherlands

J. Vergés, M. Marzo, J. A. Muñoz, E. Roca and J. Cirés

Department of Geology, University of Barcelona, Barcelona, Spain

R. Zoetemeijer and S. Cloetingh

Faculty of Earth Sciences, Vrije University, Amsterdam, the Netherlands

C. Puigdefabregas

Geological Survey of Catalunya, Barcelona, Spain

Received 15 October 1994; revised 20 February 1995; accepted 9 May 1995

The results are presented of a two-dimensional flexural modelling study of the lithosphere underlying the southern Pyrenees and the Ebro Basin. The modelling is based on a crustal-scale balanced cross-section along a profile through the north-eastern part of the Iberian plate. Two time slices of the structural evolutions of the mountain chain are modelled: the present day configuration and the configuration at Middle Lutetian time (47 Ma), where important structural and sedimentological changes are observed. The flexure model incorporates lateral variations in the effective elastic thickness (EET) of the lithosphere. The present day deflection in the profile is simulated using boundary forces and a northward decreasing EET that varies from 30 to 11 km. Models for Middle Lutetian times indicate EET values of 26–18 km in the northern part of the profile, assuming that the EET at the distal margin of the Ebro Basin has not significantly changed since Middle Lutetian times. These higher values for the EET at Middle Lutetian times suggest that the effect of the Cretaceous extensional phase on the present day flexural rigidity is small and, therefore, the inferred northward decreasing rigidity is predominantly related to the Pyrenean collision. Flexural modelling provides also constraints for the palaeo-elevation of the inner part of the chain. Including the assumption that the EET at the distal margin of the Ebro Basin has not significantly changed since Middle Lutetian times, the model predicts a maximum palaeo-elevation of ~2000 m, which is in agreement with geological observations concerning the relation between basin-fill and palaeo-elevation.

Keywords: palaeo-elevation; flexural modelling; effective elastic thickness

As demonstrated by several studies during the last decade (e.g. Beaumont, 1981; Flemings and Jordan, 1989; Sinclair *et al.*, 1991), the flexural history of the lithosphere exerts a strong influence on the strati-

graphic development of foreland basins. Of specific interest in this respect is the spatial distribution and temporal evolution of the lithospheric rigidity. Expressed in the effective elastic thickness (EET), the lithospheric rigidity largely depends on the dynamic balance between the lithospheric structure, topo-

* Correspondence to Dr H. Millán

graphic load and intraplate (boundary) forces (Burov and Diament, in press).

Royden and Burchfiel (1989), Royden (1993) and Doglioni (1993) have proposed that thrust belts developed at continental subduction boundaries can be divided into two distinct classes depending on the rates of subduction and large-scale plate convergence. This classification is based on significant differences in structure, topographic elevation, metamorphism, sedimentation and also by differences in the influence exerted by the topographic and subsurface loads on the compensation of the foreland lithosphere flexure.

In the present paper we present the results of flexural modelling of a profile through the south-eastern Pyrenees and Ebro Basin (Figure 1). The construction of a balanced crustal-scale section of the Pyrenees orogen for Middle Eocene time by Vergés *et al.* (this issue) forms the basis for our flexural analysis (Figure 2a). We analyse the relative contributions of topographic and subduction loads on the present day deflection and deflection at the Middle Lutetian time. Our approach yields insights in the temporal and spatial changes in EET in the north-eastern part of the Iberian flexural plate, as well as in the changes in topographic and subsurface loads at the intra-continental subduction boundary.

Tectonic setting

The southern Pyrenean foreland basin is located on the north-eastern Iberian Peninsula, surrounded by three mountain chains, the Pyrenees to the north, the Catalan Coastal Ranges to the south-east and the Iberian Cordillera to the south-west (Figure 1). The structural development of the three chains, which evolved during the N–S convergence of the Iberian and the Eurasian plates, strongly controlled the sedimentation and geometry of the basin from late Cretaceous to Oligocene–Early Miocene times (Puigdefàbregas and Souquet, 1986; Guimerà and Alvaro, 1990; Casas Sainz, 1992).

Continent–continent collision resulted in the subduction of the lower crust and lithospheric mantle of Iberia below the Eurasian plate (ECORS-Pyrenees Team, 1988). In this tectonic framework the Pyrenees

formed at the intra-continental plate boundary, whereas the growth of the Catalan Coastal Ranges took place at the interior of the Iberian plate.

The Pyrenean orogeny was characterized by a slightly oblique collision with an onset of deformation commencing earlier in the east than in the west (Plaziat, 1981; Puigdefàbregas and Souquet, 1986). The E–W trending orogen is constituted by a double-verging wedge developed by foreland propagating thrusts at Late Cretaceous to Miocene time (Seguret, 1972; Fischer, 1984; Vergés and Martínez, 1988; Puigdefàbregas *et al.*, 1992). During this compressional period thrust sheets containing basement rocks as well as Mesozoic and Tertiary cover were translated to the north and south over the autochthonous parts of the Aquitaine and the Ebro Basins, respectively (Cámara and Klimowitz, 1985; Souquet and Peybernés, 1987; Martínez Peña and Pocoví, 1988; Baby *et al.*, 1988). Within the Catalan Coastal Ranges, the Alpine orogeny was mainly dominated by strike-slip tectonics (Guimerà, 1984). The most distinctive structural features of the range are basement-involved, NE to ENE striking faults which were reactivated with a sinistral movement from Late Cretaceous to Oligocene times (Anadón *et al.*, 1985; Roca and Desegaulx, 1992). During the Late Oligocene–Early Miocene, the western Mediterranean area was subject to NW–SE extensional tectonics (Roca and Guimerà, 1991; Roca and Desegaulx, 1992), probably related to north-west directed subduction of the African plate beneath Iberia (Boccaletti and Guazzone, 1974; Horvath and Berckhemer, 1982). During this time period the structure of the Catalan Coastal Range was strongly controlled by inherited structures of the previous compressive phase (Fontboté *et al.*, 1990). The present day Catalan margin is characterized by a general uplift and a well-developed horst and graben structure that extends to the south-east in the Valencia Trough. This Plio-Quaternary uplift caused a regional north-west tilting of the south-eastern part of the Ebro Basin (Vergés, 1993) and is probably related to the formation of a rift shoulder in the Catalan margin domain and to detachment of subducted slabs in Mediterranean area (Janssen *et al.*, 1993).

Before the Alpine orogenic period, the Pyrenean and the Catalan domains were affected by extensional tectonics often controlled by Hercynian structures (Puigdefàbregas and Souquet, 1986; Sálas, 1987; Roca, 1992). This distensional period was mainly related to the sinistral transtensional movement of Africa with respect to Eurasia from the Late Triassic to Middle Cretaceous (Ziegler, 1989; Srivastava *et al.*, 1990). Later on, during the compressive stages, tectonics were strongly influenced by Hercynian and Mesozoic pre-orogenic structures. This was especially significant in the Pyrenees, where the inherited Mesozoic faults controlled the geometry and size of the first cover thrust sheets (Martínez Peña, 1991).

The North Pyrenean Fault, crustal-scale fault, developed during the sinistral displacement of Iberia in Middle Albian to Early Cenomanian (Debroas, 1987; 1990). The structure has been interpreted as the axis of the collision belt and the present day boundary between Iberia and Europe (Choukroune, 1976; Mattauer, 1985). Support for this interpretation was

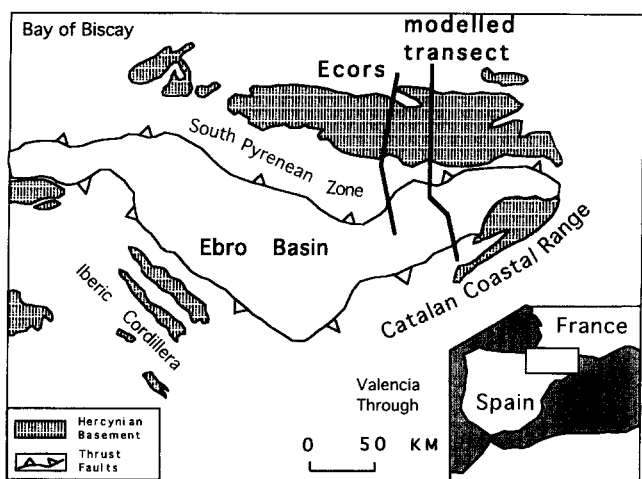


Figure 1 Location of the Ebro Basin and the main tectonic units in the area (modified after Vergés *et al.*, this issue)

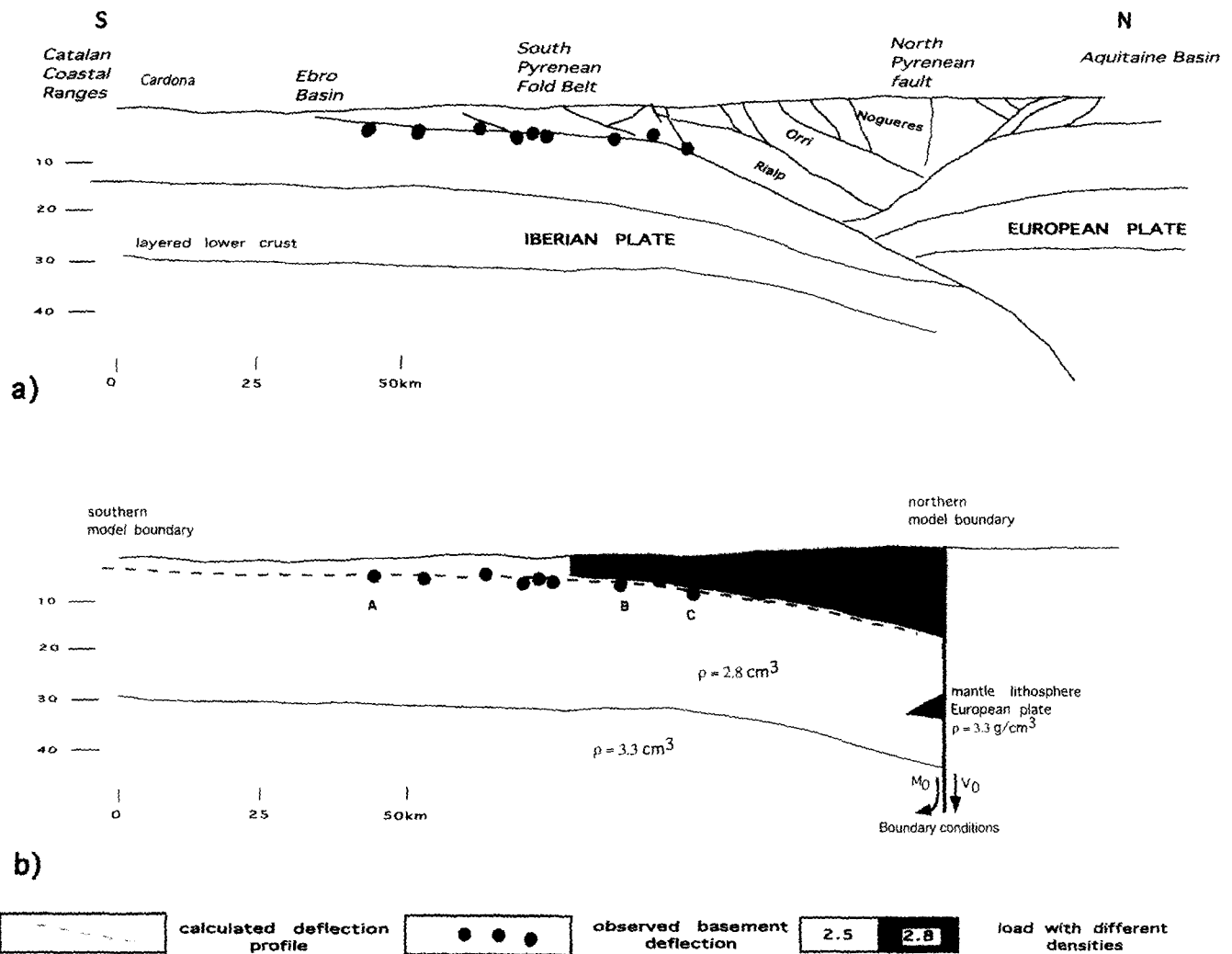


Figure 2 (a) Simplified cross-section of modelled profile. Location given in *Figure 1*. More detail and a complete balanced cross-section are given in Vergés *et al.* (this issue). Deep crustal architecture is based on results of ECORS (ECORS-Pyrenees Team, 1988). Black dots indicate the base of the Palaeocene, assumed to be the first infill of the foreland basin. (b) Calculated deflection profile. Two different grey scales represent two different densities for the load. The free boundary of the model is placed at the outcropping trace of the North Pyrenean Fault. Boundary conditions: M_0 (bending moment) and V_0 (shear force). Between point A (southernmost data point) and point B a gentle basement dip is observed and between point B and C (northernmost data point) a steeper dip is observed

obtained from seismic refraction data showing a drastic change in Moho depth below the trace of the North Pyrenean Fault (Daignieres *et al.*, 1982). However, following the completion of the ECORS deep seismic reflection profile, this interpretation has been questioned as it appears that at present the fault is cut at depth by the North Pyrenean basal thrust (ECORS-Pyrenees Team, 1988; Roure *et al.*, 1989; Muñoz, 1992).

Model description

The deflection of the Iberian plate is modelled adopting a semi-infinite elastic plate overlying an inviscid substratum incorporating lateral variations of EET (Bodine, 1981). In our modelling approach (see Zoetemeijer *et al.*, 1990; 1993), the deflection of the elastic plate occurs in response to topographic loading and plate boundary forces. In the model a theoretical Bouguer gravity anomaly is calculated, generated by the density distribution resulting from the bending of the plate. Comparing these inferred anomalies with

Bouguer gravity anomaly data gives an independent control on the amount of flexural subsidence.

The calculated deflection is compared with the present position of the base of the Palaeocene deposits in the autochthonous part of the Ebro Basin (Berastegui *et al.*, 1993). These deposits correspond to the first infill of the foredeep basin along most of the southern part of the foreland lithosphere. The position of its base is constrained by seismic reflection data (*Figure 2*). The deflection underneath the Pyrenees is more difficult to constrain. Note that the curvature of the detachment level, as can be observed from *Figure 2a*, is not the curvature due to lithosphere deflection. The curvature of the Moho, however, is a good indicator and, therefore, the amount of deflection is derived from the present depth of the Moho minus the crustal thickness measured from the restored cross-section. For the modelling of the present day situation we have excluded the southern part of the basin to avoid the effect of rift shoulder uplift related to the Neogene extension of the Catalan domain (Janssen *et al.*, 1993; Vergés, 1993). Field data suggest that the effect of rift

shoulder uplift is negligible north of Cardona (Vergés, this issue) and, therefore, we restricted the analysis of the flexure to the area north of this locality (Figure 2a). The northernmost extremity of the subducted lower crust which experienced the most intensive extensional deformation (see Vergés *et al.*, their Figure 2, this issue) is not included in the modelling, in the absence of geophysical control on its present day state and position.

We defined the northern model boundary of the elastic plate by a vertical line coinciding with the North Pyrenean Fault at the surface (Figure 2b). As mentioned earlier seismic data (Choukroune *et al.*, 1989) show that the continuation of the structure at depth is uncertain. Gravity data, however (Torné *et al.*, 1989), indicate a gravity minimum at this location, implying lateral density changes at depth. The

modelling takes into account the gravimetric and subload effects of a triangular-shaped part of upper mantle corresponding to the European lithosphere. This mantle segment overrides the down-going Iberian plate and lies within the limits of the model (Figure 2a and 2b). An alternative scenario with a plate boundary defined at the southernmost limit of the European plate (Figure 2a) underestimates the loading of the Iberian plate and overestimates the elastic support of the European plate.

Gravity data used as a constraint for the modelling are obtained from the Bouguer anomaly map of Catalunya (Casas *et al.*, 1987). In the following we use different densities for the calculation of the topographic load (i.e. the load produced by thrusting and basin infill); see Figure 2. The constraint density zones are

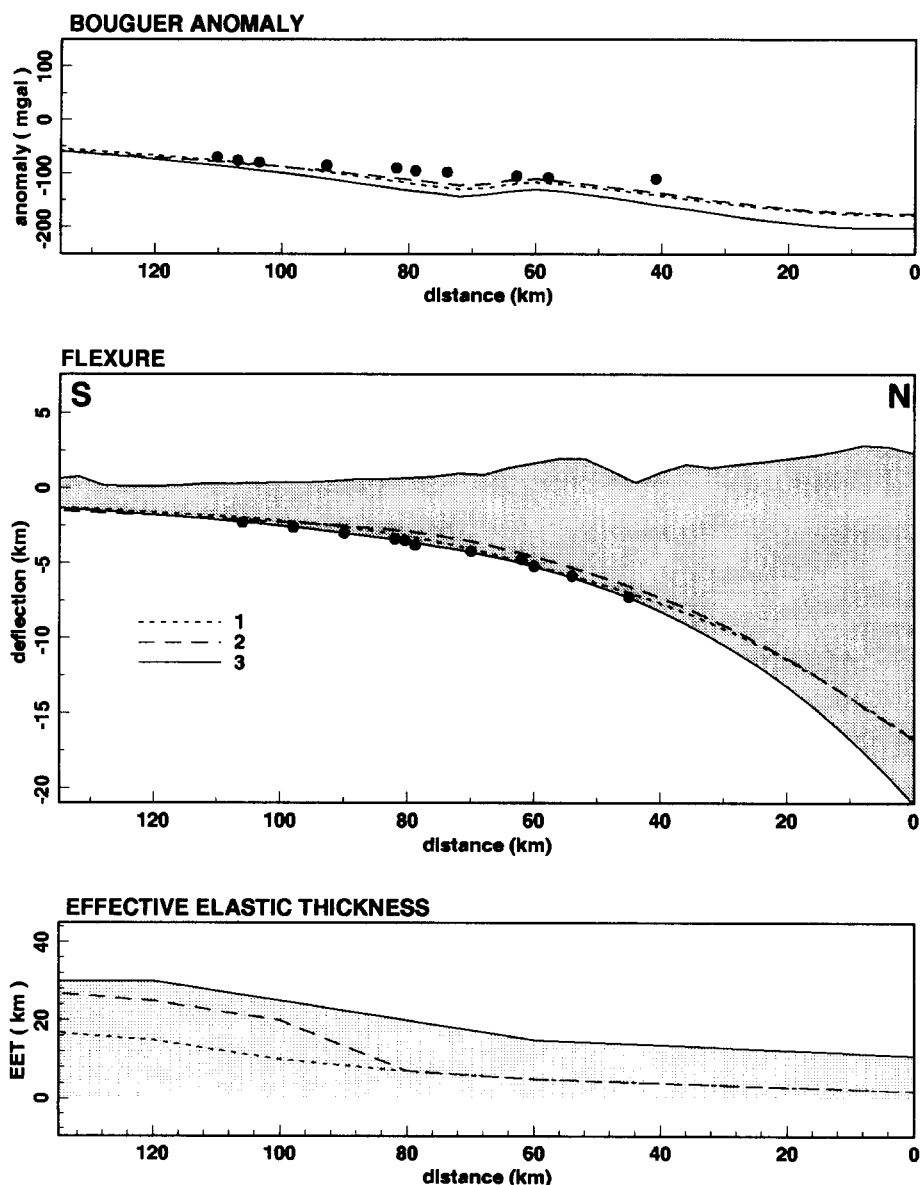


Figure 3 Model results for the present day situation using three different subduction loading scenarios: (1) $M_0 = 0.0 \text{ N}$, $V_0 = 0.0 \text{ N/m}$ and relatively low EET values; (2) $M_0 = 0.0 \text{ N}$, $V_0 = 0.0 \text{ N/m}$ and intermediate EET values; and (3) $M_0 = 8.0 \times 10^{16} \text{ N}$, $V_0 = 2.0 \times 10^{11} \text{ N/m}$ and relatively high EET values. Dots represent gravity and reflection data. Upper panel: gravity anomalies predicted by the three model scenarios. Realistic estimates of the density of infill in the model do not lead to a fit with observed Bouguer anomalies. An intracrustal higher density layer is adopted as a possible explanation. Middle panel: deflection profiles resulting from the three different model scenarios. For the scenarios with zero M_0 and V_0 a fit is not obtained, even for very low EET values. Lower panel: EET variations for the three different computed deflections. All EET values are decreasing towards the north

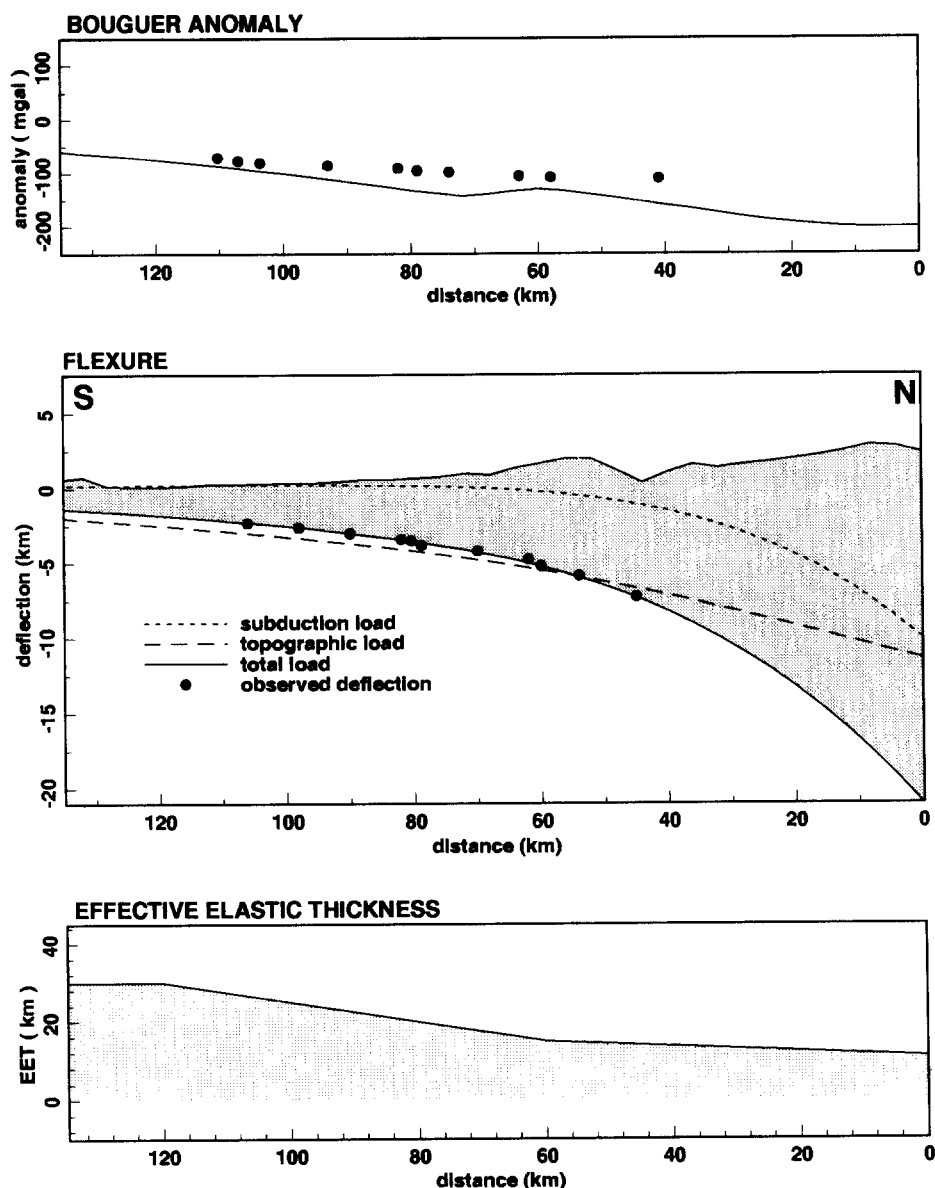


Figure 4 Relative contributions of subduction and topographic loading. Upper panel: gravity anomalies predicted by the best flexural fit of Figure 3 (scenario 3). Middle panel: contribution of topographic loads is dominant relative to contribution of subduction loads ($M_0 = 8.0 \times 10^{16}$ N, $V_0 = 2.0 \times 10^{11}$ N/m). Lower panel: EET values for the model with the best flexural fit of Figure 3 (scenario 3)

divided by a vertical line, indicated by different shading in Figure 2b. We adopt a density of 2.8 g/cm^3 for the Palaeozoic rocks and crustal materials involved in thrusting. A density of 2.5 g/cm^3 is adopted for the Mesozoic rocks and Tertiary basin infill. We assume crustal and mantle densities of 2.8 and 3.3 g/cm^3 , respectively.

Flexural modelling results

Present day profile

The present day geological section is shown in Figure 2. The southern part of the foreland lithosphere gently dips from the southernmost datapoint (point A in Figure 2b) towards the Pyrenees, reaching a depth of 4400 m below sea level at 59 km from the northern edge of the model (point B in Figure 2b). To the north of point B the basement dips more steeply, interpreted from seismic sections to a maximum depth of ~ 7250 m below sea level (point C in Figure 2b).

Approximation of the general pattern of the deflection (Figure 3) by models with zero moment or force at the free boundary requires unreasonably low values of EET over a large area of the Iberian plate. It should be noticed that without information about basement depths from the northernmost part of the profile, the data could have been matched without requiring any subload forces at the free end of the plate or the need of significant reduction of the EET towards the north (see Zoetemeijer *et al.*, 1990).

Taking the data for the present day profile into account, the best-fitting deflection was obtained for a model with a decreasing EET towards the north and sub-crustal forces at the plate boundary (Figure 3). The northward decreasing flexural rigidity is consistent with the results based on a cross-section located westward of the present study (Brunet, 1986). The southern and undeformed part of the foreland lithosphere is characterized by EET values of 30 km. In the northern part of the plate EET values decrease to 11 km (Figure 3).

The plate boundary conditions support values for a bending moment of 8.0×10^{16} N and a vertical shear force of 2.0×10^{11} N/m (Figure 4). These values are relatively low compared with estimates obtained from other mountain chains developed at continental plate boundaries (Royden, 1993).

The average thickness of the Iberian crust is 31 km (Banda, 1987). The calculated gravity profile shows a downward shift in relation to gravity anomaly observations. This discrepancy extends along the whole model, increasing towards the area of maximum flexure. As more realistic densities for the Tertiary infill (2.45 g/cm^3) and the Mesozoic cover (2.65 g/cm^3) do not alter the computed gravity significantly, the misfit between the calculated and observed anomalies is probably the result of an intra-crustal higher density layer, as suggested by Torné *et al.* (1989) for the ECORS-Pyrenees transect, 50 km west to the present study. The step in the computed gravity observed in the present day profile is due to the sharp transition between the lower densities used for the sedimentary infill/Mesozoic rocks and the higher densities of the basement thrust sheets. The predictions of the gravity model do not take into account the contribution of the density distribution in the European plate. Therefore, the calculated gravity anomaly in the area within 10 km of the northern plate boundary is not realistic.

Middle Lutetian palaeo-elevation

Structural and stratigraphic data, together with palaeo-botanical assemblages and palaeo-geographical reconstructions, allow the construction of a partially restored crustal-scale cross-section for Middle Lutetian times (Vergés *et al.*, this issue). The analysis of the Middle Lutetian lithospheric deflection was prolonged southward, a few kilometres offshore under the Mediterranean Sea, in the absence of geological evidence for interference by other tectonic processes with the foreland basin development before this time slice.

The reconstruction of the geometry of the basin provides a good control on the deflection of the base of the Palaeocene as determined in the present day section. Reconstruction of the horizontal extent of the subaerial palaeo-topography is constrained by the continental-marine transition of Middle Lutetian sediments. The southern limit between marine and continental infill of the Middle Lutetian basin (Puigdefàbregas *et al.*, 1986) is located 150–170 km south of the northern limit of the flexural model (Figure 2b). At the same time, the syn-tectonic shallow marine sediments related to the front of the Noguères thrust sheet indicate submarine conditions of the more external parts. The Lutetian topography is assumed to have a maximum elevation (water divide) situated near the leading edge of the non-subducted European plate, based on experimental and analytical models that consider partial lithospheric subduction (Malavieille, 1984; Knoons, 1990; Quinlan *et al.*, 1993).

For a partially restored cross-section the inferred structural topography is, of course, always less than the palaeo-elevation. For the internal part of the chain, the available limited geological data suggest a relatively low relief (Vergés, 1993). To obtain a first estimate of the palaeo-elevation we examined the relationship

between the elevation at Lutetian times and Lutetian basin-fill. In principle, having control on sediment provenance, the amount of erosion can be determined from its time-equivalent basin-fill. In the absence of such control three possible relations can be assumed between basin-fill and palaeo-elevation (Figure 5): (1) eroded topography equals basin-fill (Figure 5 upper panel); (2) the basin-fill exceeds the amount of eroded topography, which implies that part of the fill is derived elsewhere (Figure 5, middle panel); and (3) basin-fill is less than the eroded topography, assuming that part of the sediments from the eroded topography are deposited elsewhere (Figure 5, lower panel). In favour of the 'eroded topography equals basin-fill' scenario is the fact that the southern-eastern Pyrenean foreland basin (Ripoll Basin) was closed during Cuisian and Lutetian times (Puigdefàbregas *et al.*, 1986; Vergés *et al.*, 1992). For such a scenario in which the mass of the eroded palaeo-elevation equals the Lutetian basin infill (40 km^2), the palaeo-elevation is estimated to be about 2000 m (Vergés, this issue).

If we assume that the EET for the distal sectors of foreland basins represents an inherited feature which is not modified significantly by orogenic loading (Kominz and Bond, 1986), the wide range of possible topographic elevations may be narrowed. In this instance, EET values are most similar between the present day and the partially restored sections (≈ 30 km for the same area of the less deformed sector of the plate (i.e. coordinates: $x = 110\text{--}130$ km for the present day section; $x = 150\text{--}170$ km for the partially restored section); see Figures 3 and 6b. This argument and the geological constraints mentioned earlier suggest that the most plausible maximum palaeo-elevation should range between 2000 and 1000 m. This result appears to be consistent with the low relief expected for the Middle Lutetian time.

The different models for the Middle Lutetian Ebro Basin predict a position of the peripheral bulge slightly south of the profiles shown in Figure 6, in the surroundings of the actual location of the Catalan Coastal Ranges. These results suggest that the lack of Upper Cretaceous–Middle Lutetian sediments in the Valencia Trough (Stoekinger, 1976; Roca, 1992; Roca and Desegaulx, 1992), south-east of the Catalan Coastal Ranges, could be due to the subaerial exposure of this region.

Spatial and temporal variations in EET

Comparison of the present EET values calculated for the northern sector of the Iberian plate (northward decreasing to 11 km at the plate edge) with the EET values for the partially restored profile at Middle Lutetian time (Figure 6b), reveals a decrease in the EET at this sector overprinting an inherited weakening produced by the Cretaceous extensional phase.

From the Middle Lutetian onwards the crust in the modelled transect is thickened (e.g. Seguret and Daignières, 1986; ECORS-Pyrenees Team, 1988; Roure *et al.*, 1989), the topography has increased (Vergés *et al.*, this issue) and the lithosphere is more curved (Muñoz, 1992; Vergés *et al.*, this issue). As each of these tectonic processes and structural features can lead to localized reduction of EET values (e.g.

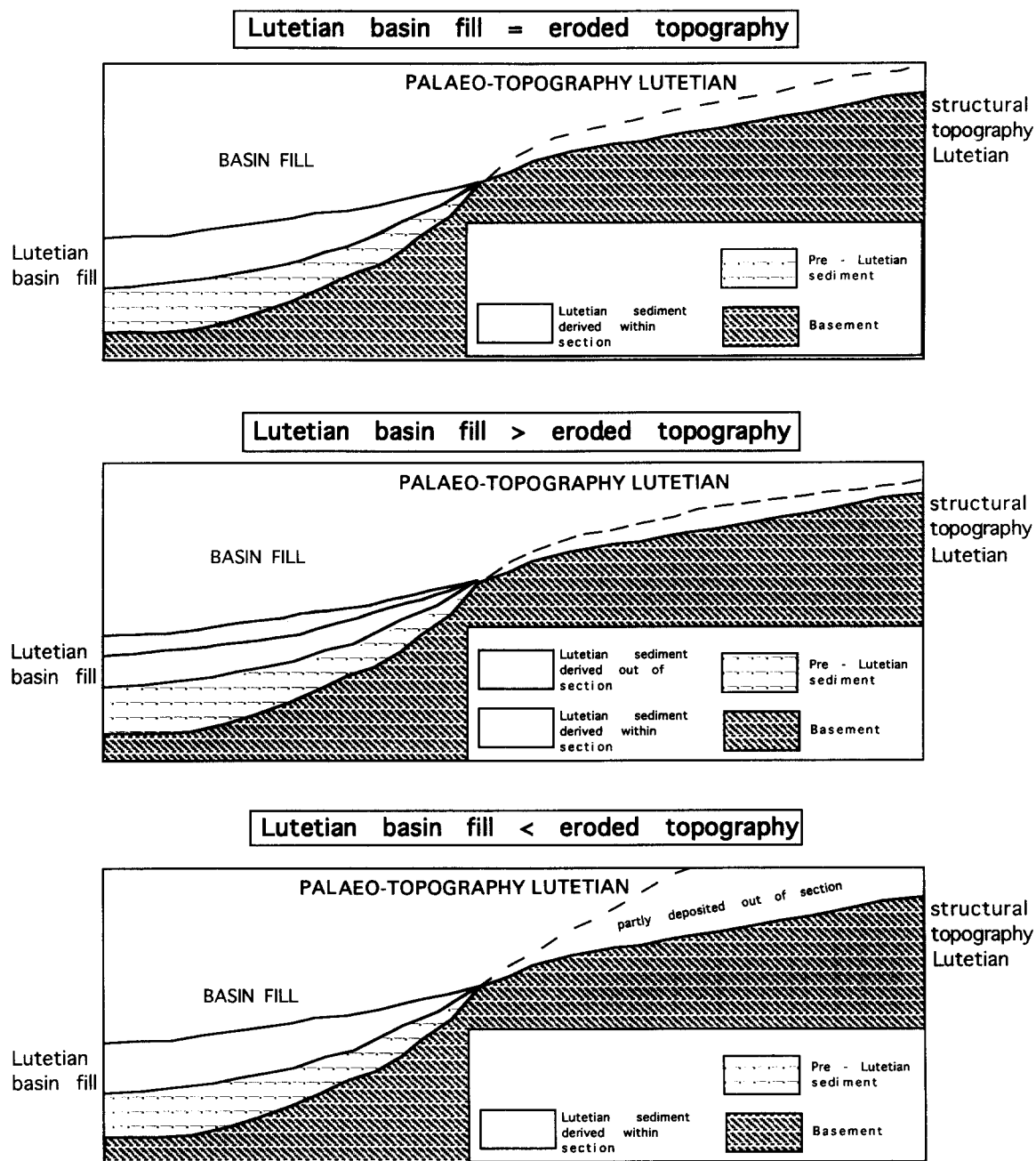


Figure 5 Schematic diagram showing three main relationships between the structural topography, palaeo-elevation and basin-fill. Upper panel: mass of basin-fill equals mass of eroded topography. Middle panel: a lower palaeo-elevation results when basin-fill is not derived from erosion of the in-plane topography, but from a source outside the section. Lower panel: a higher elevation (compared with upper panel) is produced when part of the eroded palaeo-elevation is not preserved in the basin-fill, but transported out of the section by longitudinal sediment transport.

Cochran, 1980; Cloetingh *et al.*, 1989; Burov and Diament, in press), we attribute the actual flexural rigidity distribution to one or more of these possible causes. We concluded that the decrease of EET due to the Cretaceous rifting has been overprinted by later (pre-Lutetian) tectonic processes and the possible effects of thermal history of the lithosphere have been counteracted during the compressional evolution of the orogen.

Topographic loading versus subduction loading

Royden (1993) defined advancing subduction boundaries (e.g. the Alps and the Himalayas) as those

continental convergent boundaries where the rate of overall plate convergence is greater than the rate of subduction. They are to be contrasted with retreating subduction boundaries (e.g. the Apennines) in which the rate of subduction exceeds the rate of overall plate convergence and which are also characterized by distinctive tectonic features.

The notion that a large number of geological features which characterize the orogens developed in advancing subduction boundaries (e.g. antithetic thrusting, large involvement of basement rocks in thrusting, protracted post-collisional convergence, dominance of molasse sedimentation, large amounts of erosion, large thrust sheet transport) are found in the Eastern Pyrenees

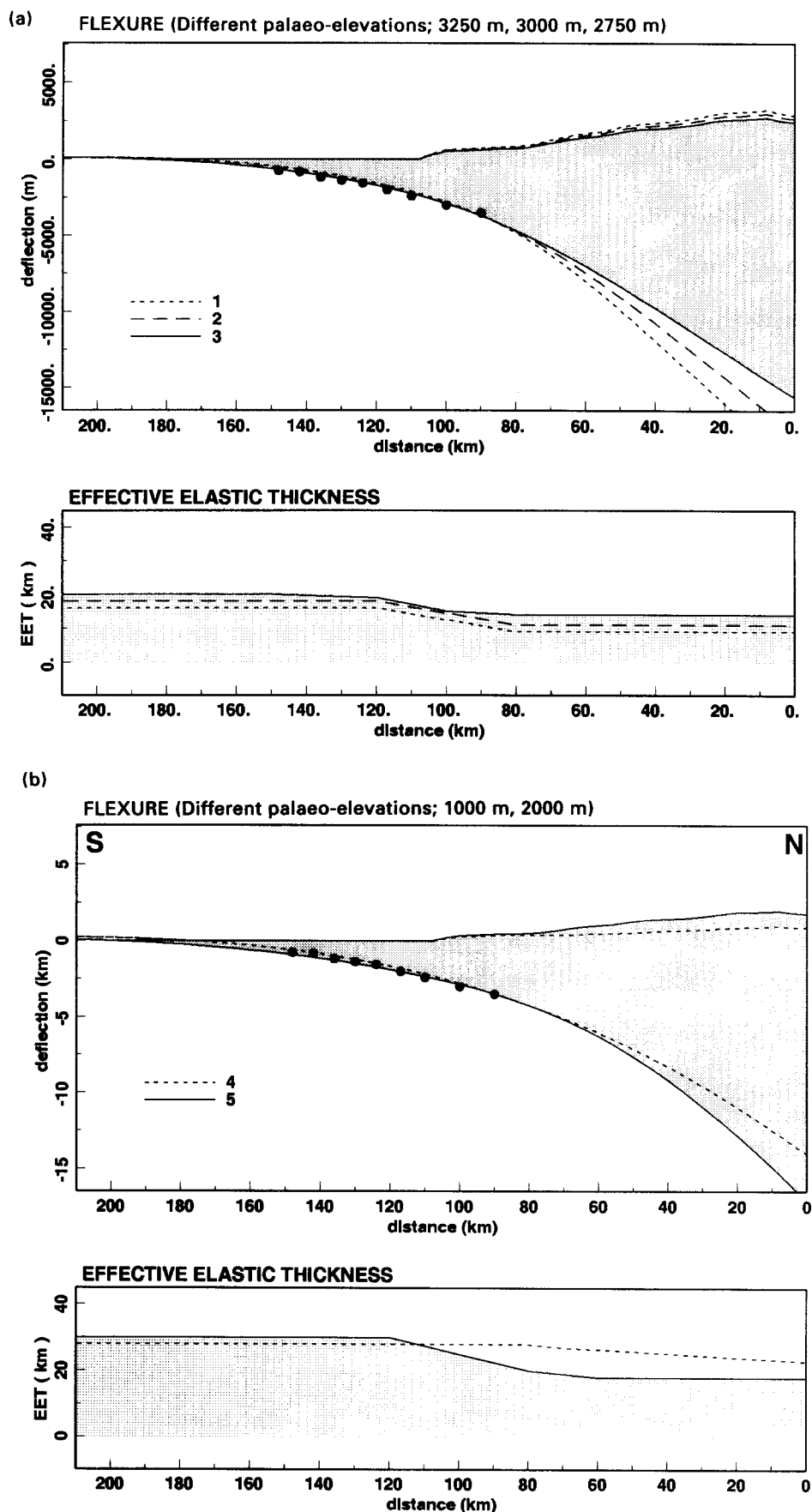


Figure 6 Modelled flexure for partly restored section (Middle Eocene) using different palaeo-elevations. Increasing elevations are accompanied by decreasing subduction forces and slightly decreasing EET values. (a) Relatively high elevations of 3250, 3000 and 2750 m, corresponding to scenarios 1, 2 and 3, respectively. Fits with decreasing EETs to the north and $M_0 = 0.0$ N and $V_0 = 0.0$ N/m. (b) Low and moderate elevations. Scenario 4: fit with 1000 m elevation, $M_0 = 7.0 \times 10^{16}$ N and $V_0 = 1.6 \times 10^{11}$ N/m. Scenario 5: fit with 2000 m elevation, $M_0 = 5.0 \times 10^{16}$ N and $V_0 = 1.0 \times 10^{11}$ N/m. Note that an overall thicker EET is required for moderate to low estimates of palaeo-elevation

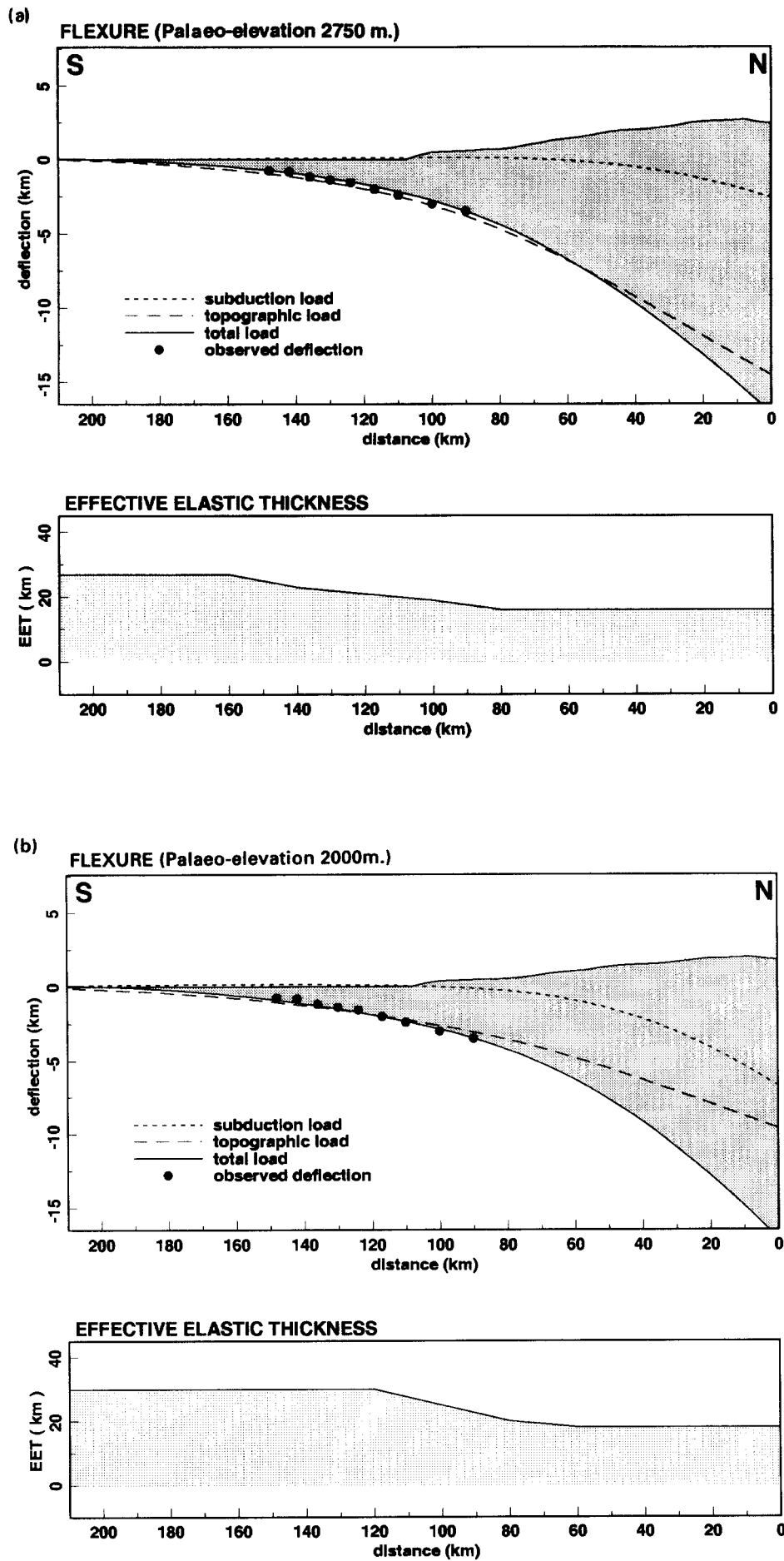


Figure 7

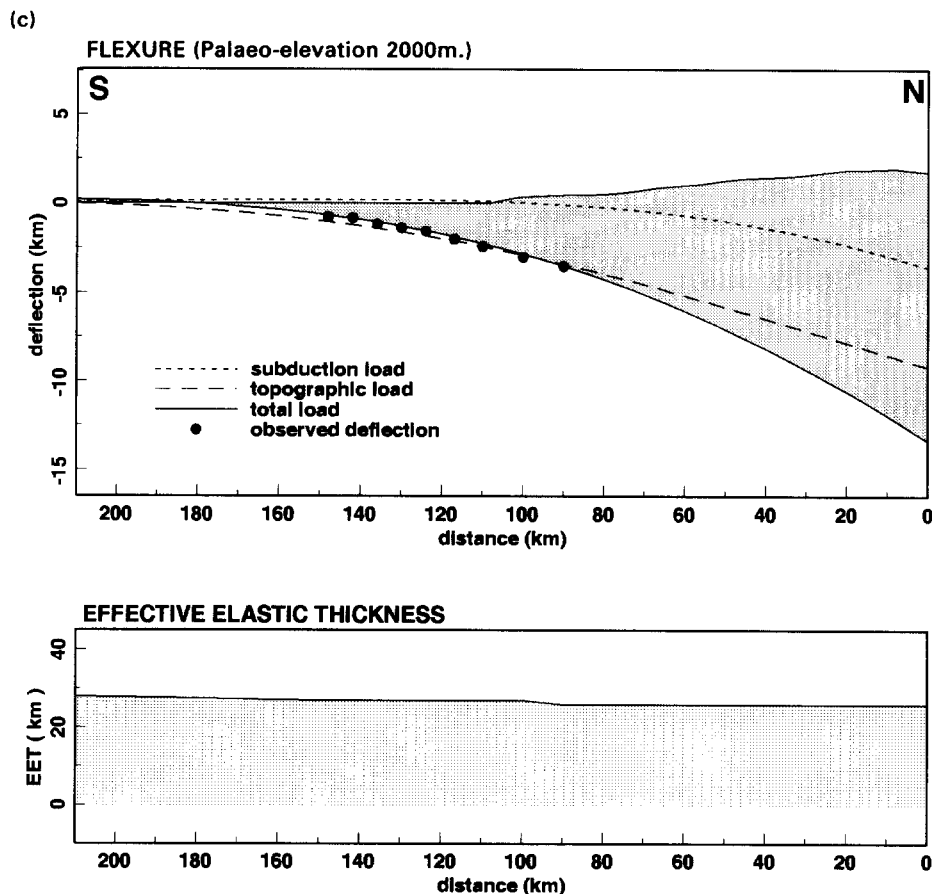


Figure 7 Comparison of relative contributions of subduction and topographic loads for different palaeo-elevations. (a) Palaeo-elevation of 2750 m and relatively low EET values, $M_0 = 3.0 \times 10^{16}$ N, $V_0 = 0.0$ N/m. As for the model results for the present day situation (Figure 4), the contribution of topographic loads is dominant relative to contribution of subduction loads. (b) Palaeo-elevation of 2000 m and relatively low EET values, $M_0 = 5.0 \times 10^{16}$ N and $V_0 = 1.0 \times 10^{11}$ N/m. (c) Resulting EET distribution for a palaeo-elevation of 2000 m assuming that the boundary conditions are similar to the present day situation ($M_0 = 8.0 \times 10^{16}$ N, $V_0 = 2.0 \times 10^{11}$ N/m). Note that higher EET values than in the present day situation (Figure 3) are required to fit the data

indicates that, at least during the last stages of its evolution, this area evolved above such a plate boundary setting.

A geological signature that also distinguishes between the end-terms of continental convergent boundaries is the part played by the topographic and subduction loads in the subsidence of a foredeep basin. At advancing subduction boundaries the deflection beneath the basin would be mainly due to the effect of the topographic load, whereas at retreating boundaries it is principally caused by subsurface loads (Royden, 1993). To investigate this point we have subtracted separately the deflection caused by each load from the total plate deflection.

Figure 4 shows an approximately linear deflection caused by the topographic load, which in turn compensates almost completely the subsidence of the southern part of the foreland lithosphere, approximately south of point B in Figure 2b. In contrast, the subduction load produces a non-linear deflection that results in an upward force acting along most of the basin and a downward force that mainly accounts for the northward increase in the curvature of the subducted plate. It therefore appears that within the framework of the plate boundary processes, the present Pyrenean continental boundary falls into the category of advancing subduction boundaries.

The flexural analysis of the Middle Lutetian selected profiles (Figure 7a and 7b) reveals that, although the topographic load plays a predominant part in the subsidence of the southern and middle part of the foreland basin, the subsidence of the remaining part of the basin and the internal parts of the thrust belt is due to the combined effects of subduction and topographic loads. Moreover, as in the present day situation, the subsurface loads cause an uplift of the southern foreland basin basement and an increase in the overall curvature of the lithospheric plate.

An approximately homogeneous EET distribution with a thickness of ≈ 27 km (Figure 7c) results when it is assumed that the palaeo-elevation was 2000 m and that the boundary conditions in the Middle Lutetian have the same values as for the present day situation. This may indicate that the low topography inferred for the Middle Lutetian time determines the subduction load to have a relatively greater importance in relation to the present day state where topography is high enough to compensate the foreland basin. Obviously, the temporal change in the part played by the topographic load can account for the increase with time of the basin infill and for the shortening of the upper crust by stacking of the basement-involved thrust sheets, which, in turn, increases the size of the area affected by the topographic load.

Conclusions

Two-dimensional flexural modelling of a crustal-scale balanced cross-section across the south-eastern Pyrenean domain demonstrates that the observed deflection of this sector of the Iberian plate can be explained by the combined effects of topographic and subsurface loads. The results presented in this paper support a scenario in which during the last stages of the Pyrenean orogeny the Ebro Basin evolved in front of an advancing subduction zone, where the subsidence of the trough was mainly controlled by the topographic load.

The present day deflection was simulated with a northward decreasing EET, varying from 30 to 11 km. The flexural modelling of the partially restored section shows that the deflection of the Middle Lutetian foreland lithosphere is controlled by both subsurface and topographic loads. In this instance, the deflection can be simulated with EET values between 30 and 18 km. For an EET of the external parts of the foreland basin, not modulated significantly by orogenic loading, palaeo-topographic elevations between 2000 and 1000 m appear to be the most plausible values for Middle Lutetian times.

The time step modelling described in this paper allows the quantitative discrimination of plausible genetic interpretations of the present day flexural strength of the lithosphere that are considered rheologically acceptable in the absence of constraints on palaeo-EET values. The decrease in EET since Middle Lutetian times is probably caused by relatively late stage orogenic processes invoking high plate curvature and thickening of the crust (McNutt *et al.*, 1988; Watts, 1992; Burov and Diament, in press). Apparently, the effect of the Cretaceous extensional phase on the present day flexural rigidity was small, as the Middle Eocene flexural rigidity of the plate is about the same or even greater than the actual rigidity. Assuming that boundary conditions and EET values at the southern margin have not changed since the Middle Lutetian, the EET distribution is approximately uniform with a thickness of 27 km.

Acknowledgements

The authors thank J. Brunet, M. Ford, E. Marsella and F. Roure for critical and constructive reviews. This research is supported by the IBS (Integrated Basin Studies) project, part of the Joulle II research program funded by the Commission of the European Communities (contract Nr. JOU2CT 92-0110) IBS Contribution No. JOU2-CT 92-0110 and Publication No. 950313 of the Netherlands Research School of Sedimentary Geology. The research was also supported by the projects DGICYT-BP91-0252 and DGICYT-PB91-0805.

References

Anadón, P., Cabrera, L., Guimerà, J. and Santanach, P. (1985) Paleogene strike-slip tectonics and sedimentation along the southeastern margin of the Ebro basin. In: *Strike-Slip Tectonics and Sedimentation* (Eds K. T. Biddle and N. Christie-Blick), *Spec. Publ. Soc. Econ. Paleontol. Mineral. No. 37*, 303–318

- Baby, P., Crouzet, G., Specht, M., Déramond, J., Bilotte, M. and Debroas, E. J. (1988) Rôle des paléostratigraphies albcénomaniennes dans la géométrie des chevauchements frontaux nord-pyrénéens *C. R. Acad. Sci. Paris* **306**, 307–313
- Banda, E. (1987) Crustal parameters in the Iberian Peninsula *Phys. Earth Planet. Interiors* **51**, 222–225
- Beaumont, C. (1981) Foreland basins *Geophys. J. R. Astron. Soc.* **65**, 291–329
- Berastegui, X., Losantos, M., Muñoz, J. A. Puigdefàbregas, C. (1993) Tall geologic del Pirineu Central 1/200.000 *Public. del Geologic de Catalunya i Institut Cartografic de Catalunya*, 62 pp
- Boccaletti, M. and Guazzone, G. (1974) Remnant arcs and marginal basins in the Cenozoic development of the Mediterranean *Nature* **252**, 18–21
- Bodine, J. H. (1981) The thermo-mechanical properties of the oceanic lithosphere, *PhD Thesis*, 332 pp
- Brunet, M. F. (1986) The influence of the evolution of the Pyrenees on adjacent basins *Tectonophysics* **129**, 343–354
- Burov, E. B. and Diament, M. The effective elastic thickness of continental lithosphere: What does it really mean? (Constraints from rheology, topography and gravity) *J. Geophys. Res.*, **100**(B3), 3905–3927
- Cámara, P. and Klimowitz, J. (1985) Interpretación geodinámica de la vertiente centro-occidental surpirenaica *Est. Geol.* **41**, 391–404
- Casas, A., Torné, E. and Banda, E. (1987) Mapa Gravimètric de Catalunya. Escala 1/500.000 *Servei Geològic de Catalunya*, ICC, Barcelona, 1–35
- Casas Sainz, A. (1992) El frente norte de las Sierras de Cameros: estructuras cabalgantes y campos de esfuerzos. Zubia, *Mográfico No. 4*, Instituto de Estudios Riojanos, 220 pp
- Choukroune, P. (1976) Structure et évolution tectonique de la zone nord-pyrénéenne (analyse de la déformation dans une portion de chaîne à schistosité subverticale) *Mém. Soc. Géol. Fr.* **127**, 116 pp
- Choukroune, P. and ECORS-Pyrenees Team (1989) The ECORS-Pyrenean deep seismic profile reflection data and the overall structure of an orogenic belt *Tectonics* **8**, 23–29
- Cloetingh, S., Kooi, H. and Groenewoud, W. (1989) Intraplate stress and sedimentary basin evolution *Am. Geophys. Union, Geophys. Monogr.* **48**, 1–16
- Cochran, J. R. (1980) Some remarks on isostasy and long-term behaviour of the continental lithosphere *Earth Planet. Sci. Lett.* **46**, 266–274
- Daignières, M., Gallart, J., Banda, E. and Hirn, A. (1982) Implications of the seismic structure for the orogenic evolution of the Pyrenean Range *Earth Planet. Sci. Lett.* **57**, 88–100
- Debroas, E. (1987) Modèle de bassin triangulaire à l'intersection de décrochements divergents pour le fossé albo-cénomaniens de la Ballongue (zone nord-pyrénéenne, France) *Bull. Soc. Géol. Fr.* **8**, 887–898
- Debroas, E. (1990) Le flysch noir albo-cénomaniens témoin de la structuration albienne à sénonienne de la zone nord-pyrénéenne en Bigorre (Hautes Pyrénées, France) *Bull. Soc. Géol. Fr.* **8**, 273–285
- Dogliani, C. (1993) Geological evidence for a global tectonic polarity *J. Geol. Soc. Lond.* **150**, 991–1002
- ECORS-Pyrenees Team (1988) The ECORS deep reflection seismic survey across the Pyrenees *Nature* **331**, 508–511
- Fischer, M. W. (1984) Thrust tectonics in the North Pyrenees *J. Struct. Geol.* **6**, 721–726
- Flemings, P. B. and Jordan, T. E. (1989) A synthetic stratigraphic model of foreland basin development *J. Geophys. Res.* **94**, 3851–3866
- Fontboté, J. M., Guimerà, J., Roca, F., Santanach, P. and Fernandez-Ortigosa, F. (1990) The Cenozoic geodynamic evolution of the Valencia trough (western Mediterranean) *Rev. Soc. Geol. Esp.* **3**, 249–259
- Guimerà, J. (1984) Palaeogene evolution of deformation in the northeastern Iberian Peninsula *Geol. Mag.* **121**, 413–420
- Guimerà, J. and Alvaro, M. (1990) Structure et évolution de la compression alpine dans la Chaîne Ibérique et Chaîne Côtière Catalane (Espagne) *Bull. Soc. Géol. Fr.* **6**, 339–348
- Horvath, F. and Berckhemer, H. (1982) Mediterranean backarc basins *Am. Geophys. Union Geodyn. Ser.* **7**, 141–173
- Janssen, M. E., Torné, M., Cloetingh, S. and Banda, E. (1993) Pliocene uplift of the eastern Iberian margin: inferences from quantitative modelling of the Valencia Trough *Earth Planet.*

- Sci. Lett.* **119**, 585–597
- Knoons, P. O. (1990) Two-sided orogen: collision and erosion from the sandbox to the Southern Alps, New Zealand *Geology* **18**, 679–682
- Kominz, M. A. and Bond, G. C. (1986) Geophysical modelling of the geothermal history of foreland basins *Nature* **320**, 252–256
- Malavieille, J. (1984) Modélisation expérimentale des chevauchements imbriqués: application aux chaînes de montagnes *Bull. Soc. Géol. Fr.* **7**, 129–138
- Martínez Peña, M. B. (1991) La estructura del límite occidental de la Unidad Surpirenaica Central, *PhD Thesis*, 380 pp
- Martínez Peña, M. B. and Pocióvi, A. (1988) El amortiguamiento frontal de la estructura de la cobertera surpirenaica y su relación con el anticlinal de Barbastro-Balaguer *Acta Geológica Hispánica* **23**, 81–94
- Mattauer, M. (1968) Les traits structuraux assentiels de la chaîne des Pyrénées *Rev. Géogr. Phys. Géol. Din.* **10**, 3–12
- Mattauer, M. (1985) Présentation d'un modèle lithosphérique de la chaîne des Pyrénées *C. R. Acad. Sci. Paris* **300**, 71–74
- McNutt, M. K., Diament, M. and Kogan, M. G. (1988) Variations of elastic plate thickness at continental thrust belts *J. Geophys. Res.* **93**, 8825–8838
- Muñoz, J. A. (1992) Evolution of a continental collision belt: ECORS-Pyrenees crustal balanced cross-section. In: *Thrust Tectonics* (Ed. K. McClay), Chapman and Hall, London, 235–246
- Plaziat, J. C. (1981) Late Cretaceous to Late Eocene paleogeographic evolution of southwest Europe *Palaeogeogr. Palaeoclimatol. Palaeoecol.* **36**, 263–320
- Puigdefàbregas, C. and Souquet, P. (1986) Tectono-sedimentary cycles and depositional sequences of the Mesozoic and Tertiary from the Pyrenees *Tectonophysics* **129**, 173–203
- Puigdefàbregas, C., Muñoz, J. A. and Vergés, J. (1992) Thrusting and foreland basin evolution in the southern Pyrenees. In: *Thrust Tectonics* (Ed. K. McClay), Chapman and Hall, London, 247–254
- Quinlan, G., Beamont, C. and Hall, J. (1993) Tectonic model for crustal seismic reflectivity patterns in compressional orogens *Geology* **21**, 663–666
- Roca, E. (1992) L'estructura de la conca Catalano-Balear: paper de la compressió i la distensió en la seva gènesi, *PhD Thesis*, 330 pp
- Roca, E. and Desegaulx, P. (1992) Analysis of the geological evolution and vertical movements in the Valencia trough area, western Mediterranean *Mar. Petrol. Geol.* **9**, 167–185
- Roca, E. and Guimerà, J. (1991) The Neogene structure of the eastern Iberian margin: structural constraints on the crustal evolution of the Valencia trough (western Mediterranean) *Tectonophysics* **203**, 203–218
- Roure, F., Choukroune, P., Berastegui, X., Muñoz, J. A., Villien, A., Matheron, P., Bareyt, M., Cámara, P. and Deramond, J. (1989) ECORS Deep seismic data and balanced cross-sections, geometric constraints to trace the evolution of the Pyrenees *Tectonics* **8**, 41–50
- Royden, L. (1993) The tectonic expression slab pull at continental convergent boundaries *Tectonics* **12**, 303–325
- Royden, L. and Burchfiel, B. C. (1989) Are systematic variations in thrust belt style related to plate boundary processes? (The Western Alps versus the Carpathians) *Tectonics* **8**, 51–61
- Sálas, R. (1987) El Malm i el Cretaci inferior entre el Massís de Garraf i la Serra de'Espadà. Anàlisi de conca, *PhD Thesis*, 345 pp
- Seguret, M. (1972) Étude tectonique des nappes et séries décollées de la partie centrale du versant sud des Pyrénées *Publ. USTELA Série Geol. Struct.* **2**, 155 pp
- Seguret, M. and Daignières, M. (1986) Crustal scale balanced cross-section of the Pyrenees *Tectonophysics* **129**, 303–318
- Sinclair, H. D., Coakley, B. J., Allen, P. A. and Watts, A. B. (1991) Simulation of foreland basin stratigraphy using a diffusion model of mountain belt uplift and erosion: an example from the Central Alps, Switzerland *Tectonics* **10**, 599–620
- Souquet, M. and Peybernés, B. (1987) Allochtonie des massifs primaires nor-pyrénéens des Pyrénées Centrales *C. R. Acad. Sci.* **305**, 733–739
- Srivastava, S. P., Roest, W. R., Kovacs, L. C., Oakey, G., Lévesque, S., Verhoef, J. and Macnab, R. (1990) Motion of Iberia since the Late Jurassic: results from detailed aeromagnetic measurements in the Newfoundland Basin *Tectonophysics* **184**, 229–260
- Stoeckinger, W. T. (1976) Valencian Gulf offer deadline nears *Oil Gas J. Mar.* **197–204**; Apr, 181–183
- Torné, M., De Cabissole, B., Bayer, R., Casas, A., Daignières, M. and Rivero, A. (1989) Gravity constraints on the deep structure of the Pyrenean belt along the ECORS profile *Tectonophysics* **165**, 105–116
- Turcotte, D. L. and Schubert, G. (1982) *Geodynamics*, Wiley, New York, 450 pp
- Vergés, J. (1993) Estudi geològic del vessant sud del Pirineu oriental i central. Evolució cinemàtica en 3D, *PhD Thesis*, Univ. Barcelona, 203 pp
- Vergés, J. and Martínez, A. (1988) Corte compensado del Pirineo oriental: geometría de las cuencas de antepaís y edades de emplazamiento de los mantos de corrimiento *Acta Geológica Hispánica* **23**, 95–106
- Watts, A. B. (1992) The effective elastic thickness of the lithosphere and the evolution of foreland basins *Basin Res.* **4**, 169–178
- Williams, G. D. and Fischer, M. W. (1984) A balanced section across the Pyrenean orogenic belt *Tectonics* **3**, 303–318
- Ziegler, P. A. (1989) Geodynamic model for Alpine intra-plate compressional deformation in the Western and Central Europe. In: *Inversion Tectonics* (Eds M. A. Cooper and G. D. Williams), *Spec. Publ. Geol. Soc. London No. 44*, 63–85
- Zoetmeijer, R. (1993) Tectonic modelling of foreland basins: thin skinned thrusting, syntectonic sedimentation and lithospheric flexure, *PhD Thesis*, Vrije Universiteit, Amsterdam, 148 pp
- Zoetmeijer, R., Desegaulx, P., Cloetingh, S., Roure, F. and Moretti, I. (1990) Lithospheric dynamics and tectonic-stratigraphic evolution of the Ebro Basin *J. Geophys. Res.* **95**, 2701–2711
- Zoetmeijer, R., Cloetingh, S., Sassi, W. and Roure, F. (1993) Stratigraphic modelling of piggyback basins: record of tectonic evolution *Tectonophysics* **226**, 253–269